

## Article

# New Approach Study on Dry Coal Cleaning System with Two-Stage Corona Electrostatic Processes for High-Sulfur Low-Grade Fine Coals

Chengyuan Liu and Qingyue Wang \* 

Graduate School of Science and Engineering, Saitama University, 255 Shimo-Okubo, Sakura-ku, Saitama 338-8570, Japan; liu.c.046@ms.saitama-u.ac.jp

\* Correspondence: seiyo@mail.saitama-u.ac.jp; Tel.: +81-(48)-8583733

**Abstract:** Corona electrostatic separation can remove inorganic materials from coal, reduce coal ash content and sulfur content and improve coal quality, reduce air pollution caused by smoke dust, SO<sub>x</sub>, and CO<sub>x</sub>. The performance of corona electrostatic separation technology in cleaning a middle ash medium-ash, high-sulfur coal was experimentally investigated. The electrode voltage, drum rotational speed, and feeding speed were tested, whereas other parameters were maintained constant during the experiment. The results indicate that the performance of this technology in cleaning medium-ash, high-sulfur coal can be improved by optimizing the process parameters. The results demonstrate that corona electrostatic separation is effective for the beneficiation of this grade coal. In addition, the efficiency of coal cleaning is significantly improved by adding the second stage beneficiation to clean the middlings out from the first stage beneficiation. In this study, the first stage of beneficiation recovered 38.00% (by weight) of clean coal (ash content below 20%), and the second stage recovered 48.58% (by weight) of clean coal, improving the overall separation efficiency from 0.69 to 1.74. Furthermore, the sulfur content was reduced from 4.71% (raw coal) to 3.53% (clean coal). Our result show that corona electrostatic separation can effectively reject inorganic sulfur from raw coal, and the two-stage separate is also very helpful for coal purification.

**Keywords:** corona electrostatic separation; medium-ash; high-sulfur; two-stage corona separation



**Citation:** Liu, C.; Wang, Q. New Approach Study on Dry Coal Cleaning System with Two-Stage Corona Electrostatic Processes for High-Sulfur Low-Grade Fine Coals. *Processes* **2021**, *9*, 1915. <https://doi.org/10.3390/pr9111915>

Academic Editor: Adam Smoliński

Received: 11 October 2021

Accepted: 25 October 2021

Published: 27 October 2021

**Publisher's Note:** MDPI stays neutral with regard to jurisdictional claims in published maps and institutional affiliations.



**Copyright:** © 2021 by the authors. Licensee MDPI, Basel, Switzerland. This article is an open access article distributed under the terms and conditions of the Creative Commons Attribution (CC BY) license (<https://creativecommons.org/licenses/by/4.0/>).

## 1. Introduction

Coal is a major energy source, accounting for approximately 27% of the world's total energy consumption [1] and plays an important role in providing energy around the world. China is extremely poor in crude oil and natural gas resources and therefore relies heavily on imports of these two energy resources [2,3] (the proportions imported being 70.9% and 34.9%, respectively). Renewable energies, such as solar, wind, nuclear, and hydraulic energies, yet cannot provide stable supplies in large quantities (renewable energy to account for 23% of global energy supply in 2106) [4]. Therefore, coal is considered a strategic energy reservoir and has played an irreplaceable role in China for a long time [5]. The quality of coal is considerably influenced by its contents of ash and sulfur [6]. CO<sub>2</sub> and SO<sub>2</sub> have important climatic implications [7] and could lead to temperature increases [8]. In China, coal accounts for more than 70% of the nation's total energy consumption [9,10], but high-sulfur coal cannot be used for producing high-quality coke and is not a good combustion fuel, furthermore, 92% of SO<sub>2</sub> emissions were from coal consumption in 2007 [11]. SO<sub>2</sub> can result in acid rain and photochemical smog [12], erode boilers [13], plant deaths, river and lake acidification, and human health hazards [14]. A recent study has shown that there was a significant positive correlation between SO<sub>2</sub> concentrations and environmentally persistent free radicals, which are similar to carcinogenic tar paramagnetic species in cigarettes that can cause DNA damage [15]. However, approximately 30% of China's coal resources have a medium to high sulfur content [16]. Therefore, reasonable

utilization of high-sulfur coal is an urgent issue [17], efforts should be made to reduce the emissions of  $\text{SO}_2$ , such as pre-combustion measures (i.e., coal beneficiation), process treatment during combustion (mainly efficiency improvements), and end-of-pipe treatment after combustion (the installation of scrubbers) [18,19].

Corona electrostatic separation is a coal separation technology that does not require the use of water, widely used to separate small-particle materials, such as separation of metallic and non-metallic minerals [20,21], recovery of metallic materials from waste electrical and electronic equipment [22,23], seed hulling [24], and coal purification [25]. Electrostatic separation is a low-cost, low-pollution technology for removing impurities.

In this study, the performance of corona electrostatic separation of medium-ash high-sulfur coal and the factors that influence the performance were experimentally investigated through conducting a series of experiments on samples of medium-ash high-sulfur coal.

In this study, the optimal conditions of electrode voltage, drum rotational speed, and conveyor speed in the experiment were discussed separately, and the reasons for the formation of the optimal conditions were analyzed separately to gain a deeper understanding of the principle of understanding electrostatic coal separation. Finally, the secondary coal separation by the optimal conditions resulted in a purer coal, but the improvement of efficiency was limited because the organic sulfur in the coal could not be removed by this method. In the future, a further step of purification can be carried out by chemical methods.

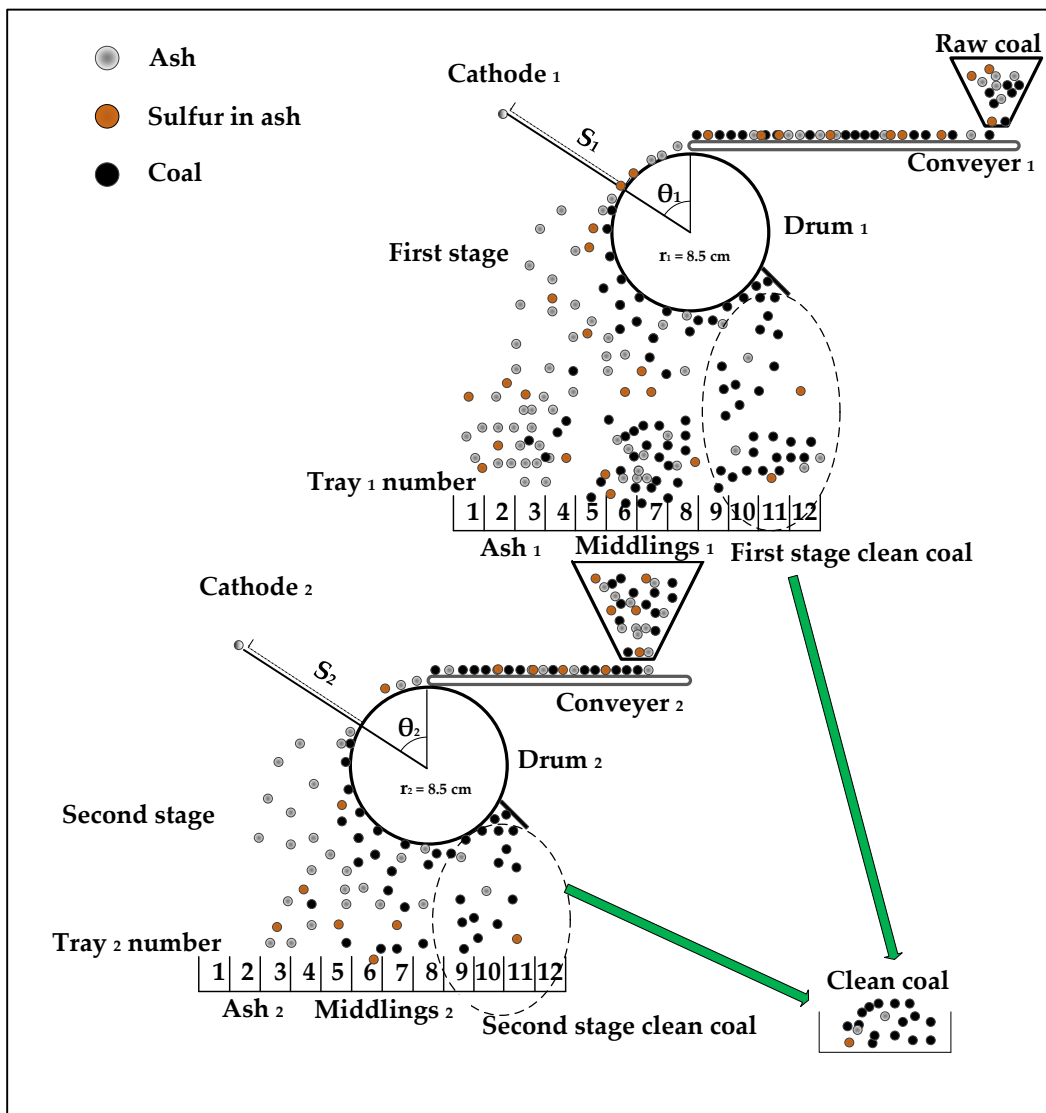
## 2. Test Samples and Methods

### 2.1. Testing Devices

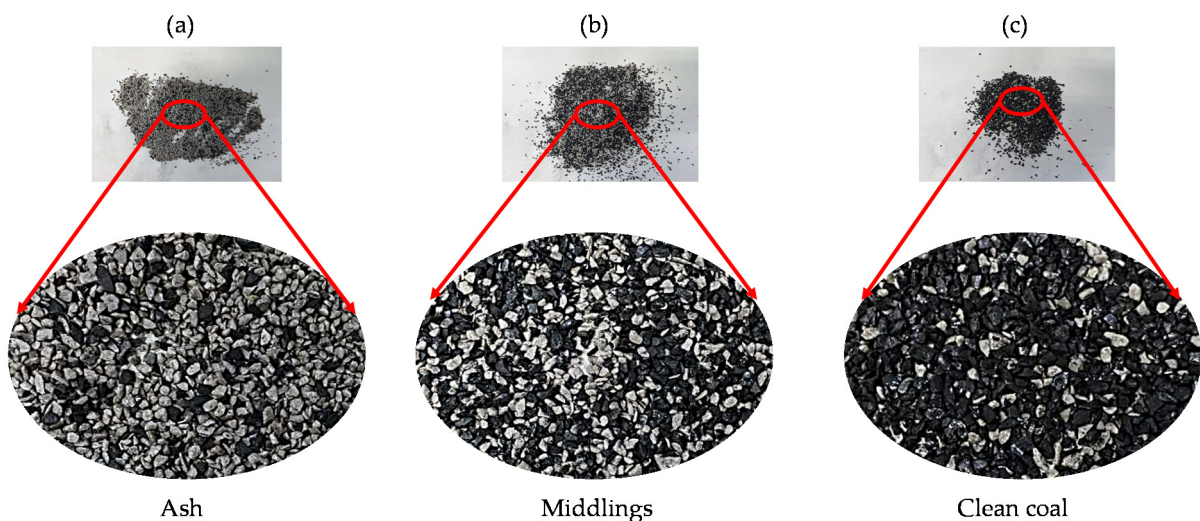
When using a corona electrostatic separator to separate coal, a considerable proportion of the separated coal is particles with an ash content of 20–60%, which are referred to as middlings. The middlings were fed into the second stage separator to improve the combustible body recovery rate and efficiency of coal beneficiation [26].

Figure 1 is a schematic illustration of the separation system, which mainly consists of a feeding funnel, conveyor, steel drum, corona electrode, and 12 equally sized collecting trays. The following process parameters were controllable: the opening size of the feeding funnel, the conveyor speed, the drum rotational speed, and the electrode voltage. The separator removes ash and sulfur from coal in the following manner. The coal fed into the feeding funnel is transferred by the conveyor onto the surface of the drum.

The electrode generates a corona discharge and electric field. Owing to the effect of the electric field force, particles of different properties will be differently charged and be subjected to different electrical field forces. In addition, different particles have different specific gravity and centrifugal force, so, the test material model experiment shows that ash and sulfur particles will fall into collecting trays on the left, while clean coal particles fall into collecting trays on the right. Different particles of ash (a), middlings (d), and clean coal (c) from the different trays are illustrated in Figure 2.



**Figure 1.** Schematic illustration of dry coal cleaning system with two-stage corona electrostatic processes for high-sulfur low-grade fine coals.



**Figure 2.** Different particles collected from different trays of separator: (a): tray numbers 1–7; (b): tray number 8; (c): tray numbers 9–12.

The separator has a maximum electrode voltage of negative ( $U_1$  and  $U_2$ ) = 30 kV. The angle ( $\theta_1$  and  $\theta_2$ ) between the line from the electrode to the center of the drum circle and the vertical line of the drum can be adjusted within the range of 30–75°. The distance ( $S_1$  and  $S_2$ ) between the electrode and drum surface can be adjusted within the range of 5–11 cm. The raw coal of approximately 100 g was fed into the separator each time. After each test, the particles collected in each of the 12 trays were weighed, and the weights were used to determine the recovery ratio of the sample. The particles collected in each tray were analyzed to determine their ash and sulfur content. The particles collected in the right trays with ash content below 20% were considered as clean coal, the particles collected in the middle trays with ash contents of 20–60% were considered as middlings and the particles collected in the left trays with ash contents above 60% were considered as tailing. The separation efficiency was computed using the following equations:

$$[SR] = \frac{(Wt_{feed} \times Sulfur_{feed\ ratio}) - (Wt_{clean} \times Sulfur_{clean\ ratio})}{Wt_{feed} \times Sulfur_{feed\ ratio}} \times 100 \quad (1)$$

$$[AR] = \frac{(Wt_{feed} \times Ash_{feed\ ratio}) - (Wt_{clean} \times Ash_{clean\ ratio})}{Wt_{feed} \times Ash_{feed\ ratio}} \times 100 \quad (2)$$

$$[CMR] = \frac{Wt_{clean} - (Wt_{clean} \times Ash_{clean\ ratio})}{Wt_{feed} - (Wt_{feed} \times Ash_{feed\ ratio})} \times 100 \quad (3)$$

$$[SE] = \frac{[AR] + [CMR] - 100}{|AR - CMR|} \quad (4)$$

SR = sulfur removal

AR = ash removal

CMR = combustible matter recover

SE = separation efficiency

$Wt_{feed}$  = mass of raw coal supply

$Wt_{clean}$  = mass of recovery of clean coal

$Sulfur_{feed\ ratio}$  = mass of sulfur rate of raw coal

$Sulfur_{clean\ ratio}$  = mass of sulfur rate of clean coal

$Ash_{feed\ ratio}$  = mass of ash rate of raw coal

$Ash_{clean\ ratio}$  = mass of ash rate of clean coal

## 2.2. High-Sulfur Raw Coal

A medium-ash and high-sulfur raw coal from China was selected for the experimental investigation. The raw coal was screened to a size range of 0.5–1 mm. Proximate analysis and ultimate analysis were performed on the raw coal particles with an analyzer of JIS M 8812: 2006 and JIS M 8819: 1997, respectively, and the sulfur content of the raw coal was determined using an HYDL-9 sulfur content analyzer (21). Table 1 shows the results of the proximate analysis and ultimate analysis. The ash content and sulfur content of the raw coal are 28.92% and 4.71%, respectively. According to the Chinese classifications of ash and sulfur contents in coal (shown in Table 2, respectively), the raw coal belonged to medium-ash, high-sulfur grade. This grade coal is difficult to use for burning because the combustion process will produce large amounts of  $SO_x$  pollution. Therefore, it is necessary to reduce the ash and sulfur in the coal.

**Table 1.** Proximate analysis and ultimate analyses of Chinese high-sulfur raw coal.

Size (mm)	Proximate Analysis (wt.%)				Ultimate Analysis (wt.%)				
	Ash	M	V.M	F.C	S	C	H	N	O
0.5–1	28.92	2.35	21.71	47.02	4.71	49.82	0.31	7.07	9.17

**Table 2.** Classification categories of ash and sulfur of coal in China [27].

Coal Grade of Ash	Ash Content ( $A_d$ ) Range/%	Coal Grade of Sulfur	Sulfur Content ( $S_d$ ) Range/%
Ultra-low-ash coal	$A_d \leq 10.00$	Ultra-low-sulfur coal	$S_d \leq 0.50$
Low-ash coal	$10.00 < A_d \leq 20.00$	Low-sulfur coal	$0.50 < S_d \leq 1.00$
Medium ash coal	$20.00 < A_d \leq 30.00$	Medium-low-sulfur coal	$1.00 < S_d \leq 1.50$
High-ash coal	$30.00 < A_d \leq 40.00$	Medium sulfur coal	$1.50 < S_d \leq 2.00$
Ultra-high-ash coal	$40.00 < A_d \leq 50.00$	High-sulfur coal	$2.00 < S_d \leq 3.00$
		Ultra-high-sulfur coal	$S_d > 3.00$

### 2.3. Experimental Methods

A three-step experimental procedure was conducted. In the first step, the coal was beneficiated using different process parameters. The major process parameters included the voltage of the electrode, the distance from the electrode to the drum, the angle between the electrode and the drum, the geometry of the electrode, the rotational speed of the drum, the speed of the conveyor, the temperature, the humidity, and the properties of the raw coal. The influences of three of the process parameters (the electrode voltage, drum rotational speed, and feeding speed) on the performance of the electrostatic separation of raw coal were investigated. To simplify the experiment, only one corona electrode was used. The factors that most influenced the electrical field were the electrode voltage, the electrode–drum distance, and electrode–drum angle. The electrical field was controlled by adjusting the voltage in the test process.

Other parameters were fixed as follows: weight of raw coal at each time: 100 g; distance between the electrode and the drum ( $S_1$  and  $S_2$ ): 7 cm; angle between the line from the electrode to the center of the drum circle and the vertical line of the drum ( $\theta_1$  and  $\theta_2$ ):  $75^\circ$ ; room temperature (T):  $25^\circ\text{C}$ ; relative humidity (RH): 60%; particle size range: 0.5–1 mm. The corona electrostatic separator had a maximum electrode voltage of 30 kV, a maximum drum rotational speed ( $R_1$  and  $R_2$ ) of 40 rpm, and a conveyor speed ( $V_1$  and  $V_2$ ) of 23 g/m (for conveying a thin layer of sample coal). At the beginning of the experiment, the drum rotational speed was set to the maximum value of 40 rpm, the conveyor speed was set to 23 g/m, and the electrode voltage was set to the maximum value of 30 kV.

During each experiment, only one of the three variable parameters changed. First, the voltage was adjusted downwardly 2.5 kV each time. The best three voltage settings were determined based on the efficiency of separation. Then, the drum rotational speed was adjusted downwardly to 10 rpm each time to investigate the performance of the separator at the optimal electrode voltage and drum rotational speeds of 40, 30, and 20 rpm. Finally, the performance of the separator at the optimal electrode voltage and drum rotational speed was observed at three different conveyor speeds: 23, 48, and 73 g/m. (Note that because accurate control of the conveyor speed was difficult, the second and third conveyor speed settings were approximately two and three times of the first setting, respectively.) Based on the data obtained, the influences of variations in the three parameters on the performance of the separator were analyzed.

In the second step, the optimal parametric settings were determined based on the performance of the separator at the different parametric settings. The middlings were fed into the separator for the second stage of separation with the optimal parametric settings. The total yield of clean coal by two stages separation was used to compute the efficiency of the two-stage separation.

In the third step, a thermogravimetric/differential thermal analysis (TG-DTA) [28] was performed on the raw coal and the clean coal of the two-stage separation using a PG 250 analyzer [29] to compare the environmental impacts of the clean coal and raw coal.

### 3. Results and Discussion

Typically, most of the inorganic sulfur can be removed during the ash removal process, as this inorganic sulfur is mainly bound to gangue particles. However, it is well known

that organic sulfur in coal is usually bound to the macromolecular skeletal structure of the organic components and is therefore difficult to remove by density separation and flotation. Therefore, desulfurization is ineffective for coals with high organic sulfur.

### 3.1. Factors Influencing Separation Efficiency

#### 3.1.1. The Influence of Electrode Voltage

The parameters were set as follows: distance ( $S_1$ ): 7 cm; angle ( $\theta_1$ ):  $75^\circ$ ; temperature (T):  $25^\circ\text{C}$ ; relative humidity (RH): 60%; rotation speed of drum ( $R_1$ ): 40 rpm; conveyor speed ( $V_1$ ): 23 g/min; the particle size range of raw coal: 0.5–1 mm. Figures 3 and 4 show the effect of separation at different electrode voltages. Figure 3a–c shows the ash ratio (%) (percentage of ash to raw coal), coal ratio (%) (percentage of coal to raw coal), and sulfur ratio (%) (percentage of sulfur to each tray) of the particles collected in the 12 trays at electrode voltages ( $U_1$ ) of 30, 27.5, and 25 kV, respectively. Coal particle weights less than 1% of that of the feedstock were not included in the analysis (their weight percentages and corresponding ash contents and sulfur contents are indicated as zero in the figures). At a voltage of 30 kV, the major particles were collected in tray numbers 7–9; at voltages of 27.5 and 25 kV, more particles were collected in tray numbers 4–8.

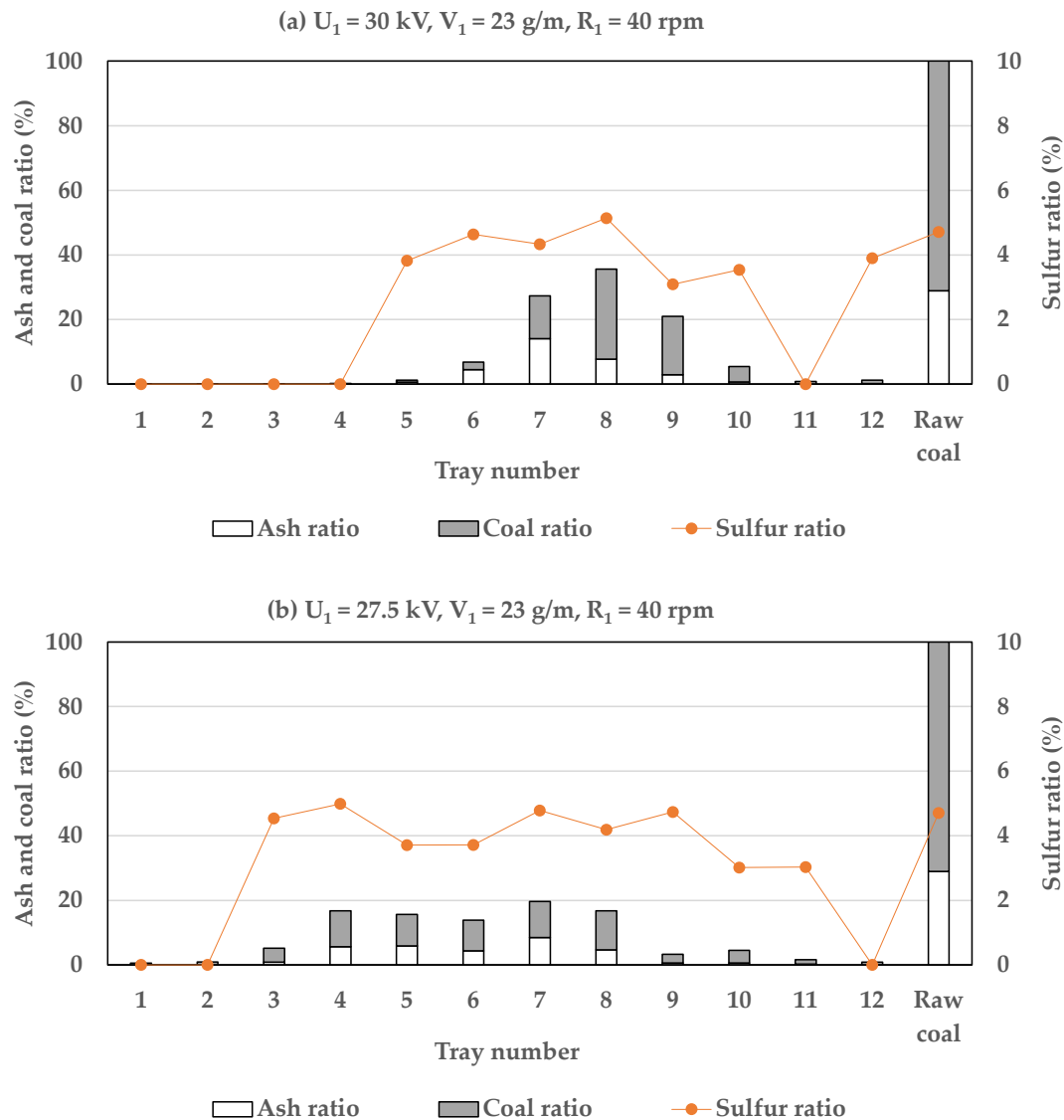
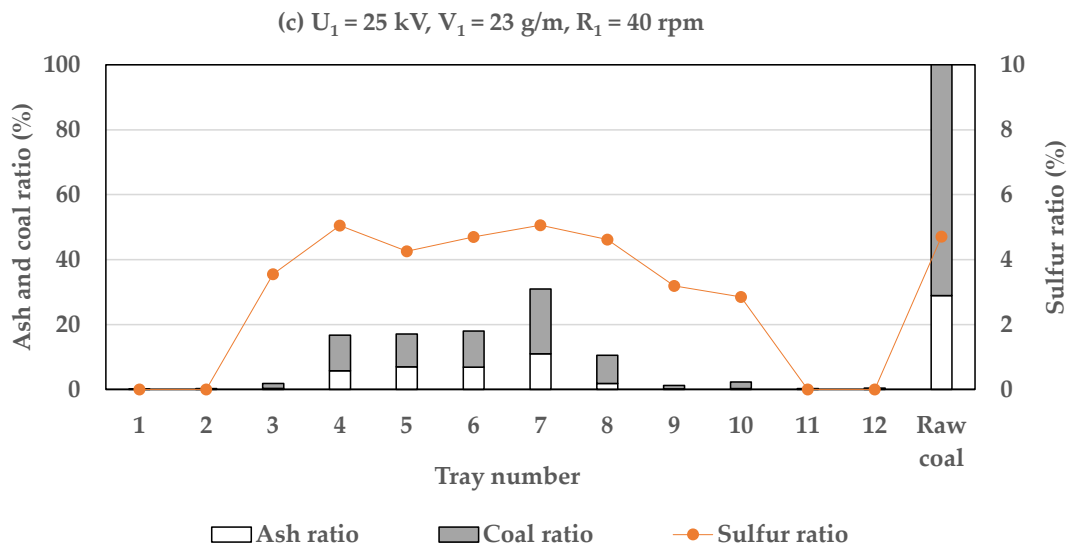
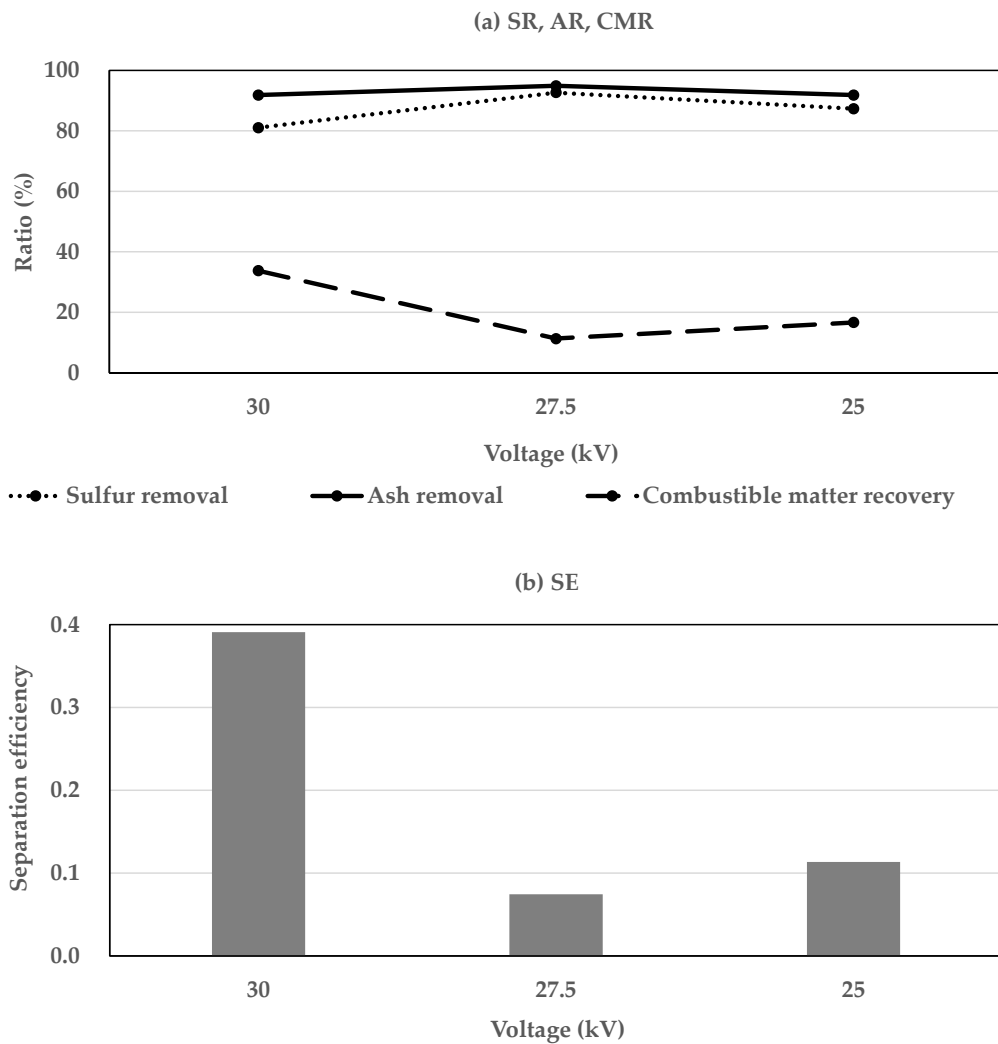


Figure 3. Cont.



**Figure 3.** Ash ratio (%), coal ratio (%), and sulfur ratio (%) of particles collected from tray numbers 1–12 at different electrode voltages: (a) 30 kV; (b) 27.5 kV; (c) 25 kV using a dry coal cleaning system with two-stage corona electrostatic processes.



**Figure 4.** Performance of coal separation at different electrode voltages: (a) ash removal ratios (%), sulfur removal ratios (%), and combustible matter recovery ratios (%); (b) efficiency of coal separation using a dry coal cleaning system with two-stage corona electrostatic processes.

A high voltage will conduct a high electric field strength, then increase the charge on the particles, and the magnitude of the force acting on the particles. Consequently, more particles adhered onto the drum surface and fell into the right trays. At a voltage of 30 kV, the particles collected from tray number 6 had the highest ash content (66.17%), followed by those in tray numbers 5–7 (ash content above 50%).

The ash content gradually decreased from tray number 8 rightward. The particles collected from tray number 8 had an ash content of 21.82% and nearly satisfied the definition of low-ash coal. The particles collected from tray numbers 9–12 had ash contents below 20% and satisfied the definition of low-ash coal (defined as clean coal in this study). In particular, the sulfur content was reduced from 4.71% to 3.09% in tray 9, and the ash content was reduced from 28.92% to 12.40% in tray 10, which has shown good experimental results.

At a voltage of 27.5 kV, the particles collected from tray numbers 9–12 also had ash contents below 20%, but their weight accounted for only 9.50% of that of the feedstock, compared with 27.75% at a voltage of 30 kV. At a voltage of 25 kV, the particles collected from tray numbers 8–12 satisfied the definition of clean coal but weighed only 14.17% of that of the feedstock. The sulfur contents of the clean coal at voltages of 30, 27.5, and 25 kV were 3.22%, 3.62%, and 4.2%, respectively. Among the three voltage settings, the 30 kV voltage resulted in the highest ash removal and combustible matter recovery ratios (Figure 4a) and the highest separation efficiency (Figure 4b). This finding is consistent with the analysis results summarized above. Therefore, at the parametric settings described at the beginning of this subsection, an electrode voltage of 30 kV resulted in the best performance of the separation of the raw coal. The performance of electrostatic separation could not be estimated when the electrode voltages were over 30 kV because of the limitations of the separator.

A low voltage will lead to low recovery ratio of combustible matter, thus leading to low separation efficiency.

### 3.1.2. The Influence of Drum Rotational Speed

Based on the tests of the influence of the electrode voltage, the test of the influences of the drum rotational speed was conducted with electrode voltage ( $U_1$ ) of 30 kV, distance ( $S_1$ ) of 7 cm, electrode angle ( $\theta_1$ ) of  $75^\circ$ , temperature of  $25^\circ\text{C}$ , relative humidity of 60%, conveyor speed ( $V_1$ ) of 23 g/min, and particle size range of raw coal of 0.5–1 mm. Figures 5 and 6 show the experimental results. Figure 5a–c shows the ash ratio (%) (percentage of ash to raw coal), coal ratio (%) (percentage of coal to raw coal), and sulfur ratio (%) (percentage of sulfur to each tray) of the particles collected from 12 trays at drum rotational speeds ( $R_1$ ) of 40, 30, and 20 rpm, respectively. The majority of the particles were collected in tray numbers 7–9 with all three drum rotational speeds. However, the ash content of the particles collected in a given tray varied with the drum rotational speed changing, and more high-purity ash particles were obtained with the drum rotational speed of 40 rpm.

However, the particles collected from tray number 8 had the largest weight (%) but had an ash content slightly exceeding 20% (21.82%) and could not be considered as clean coal, resulting in a low recovery ratio of combustible matter. The drum rotational speed of 40 rpm led to a higher ash removal ratio but a lower combustible matter recovery ratio compared with a drum rotational speed of 30 rpm (Figure 6a) and a very low proportion of middlings (which have an ash content similar to that of the raw coal). However, in this study, clean coal was defined as with ash content below 20%, and the amount of clean coal yield was used to measure the efficiency of separation, so the best setting for the drum rotational speed was judged to be 30 rpm. However, the sulfur contents of clean coal particles tested with drum rotational speeds of 40, 30, and 20 rpm were 3.22%, 4.20%, and 4.21%, respectively, which indicates that the drum rotational speed of 40 rpm will produce higher-purity clean coal and effectively reduce the sulfur content, because a higher drum rotational speed results in a larger centrifugal force, meanwhile compared with coal, mineral particles tend to lose electrical charges more easily, then the mineral particles fall from drum surface more quickly under the influence of a larger centrifugal force and a lower electric force, as a result, the particles collected from the left trays had higher ash

content and high sulfur content. In addition, a lower drum rotational speed results in a smaller centrifugal force and a lower electric force because of longer time for the particles to lose their electrical charges, so some clean coal particles fall into the middle trays.

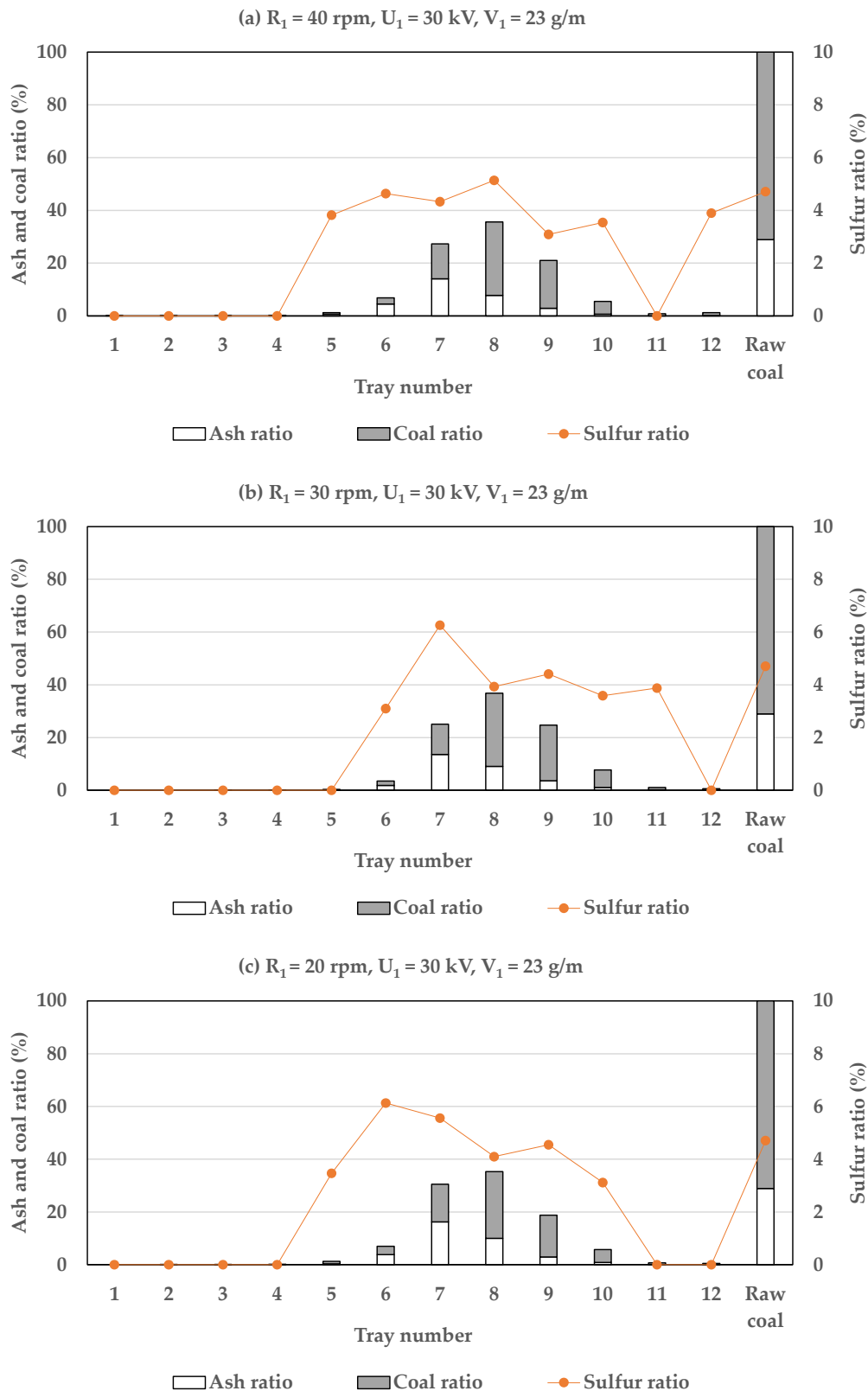


**Figure 5.** Ash ratio (%), coal ratio (%), and sulfur ratio (%) of the particles collected from the 12 trays at different drum rotational speeds: (a) 40 rpm; (b) 30 rpm; (c) 20 rpm using a dry coal cleaning system with two-stage corona electrostatic processes.

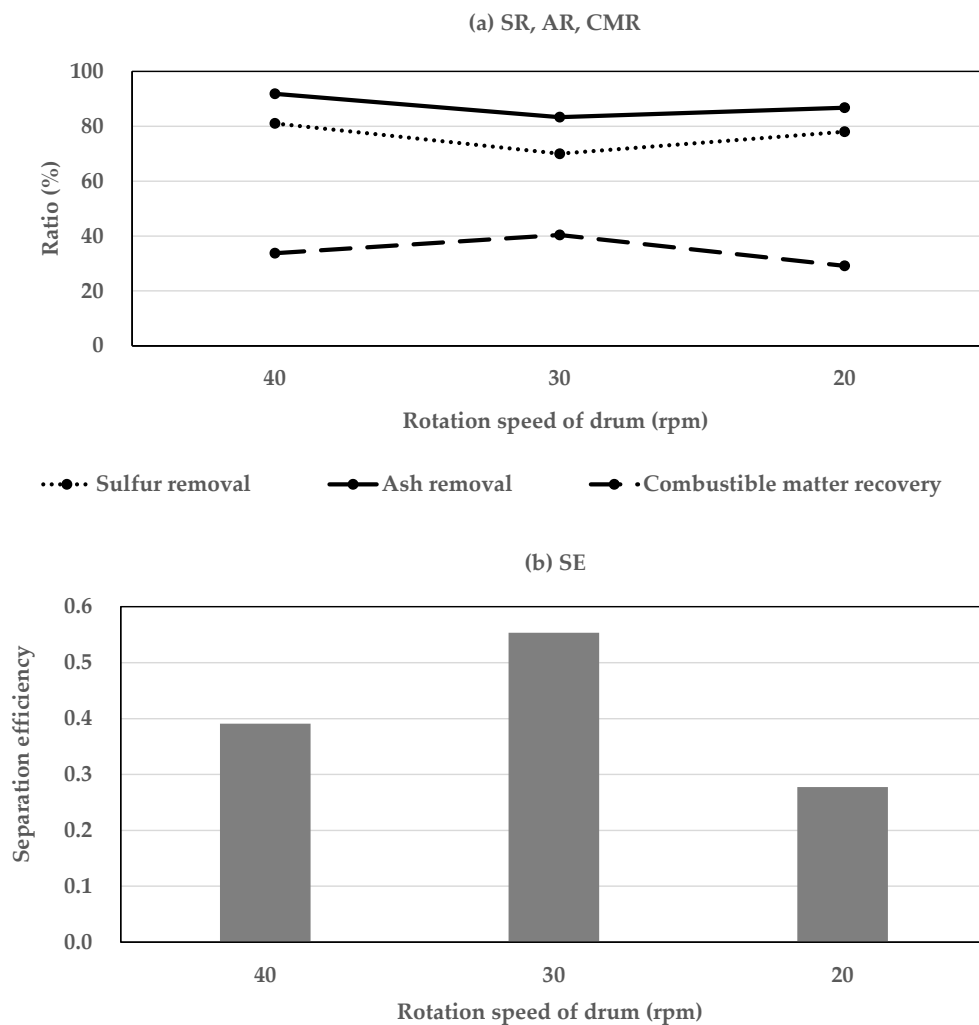


**Figure 6.** Performance of the separator at different drum rotational speeds: (a) ash removal ratios (%), sulfur removal ratios (%), and combustible matter recovery ratios (%); (b) efficiency of coal separation using a dry coal cleaning system with two-stage corona electrostatic processes.

### 3.1.3. The Influence of Conveyor Speed

Based on the tests of the influences of the electrode voltage and drum rotational speed, the influence of the conveyor speed was conducted with the optimal voltage of 30 kV, the optimal drum rotational speed ( $R_1$ ) of 30 rpm, distance ( $S_1$ ) of 7 cm, electrode angle ( $\theta_1$ ) of  $75^\circ$ , temperature of  $25^\circ\text{C}$ , relative humidity of 60%, and feedstock size range of 0.5–1 mm. The conveyor speed is an important parameter that determines the capacity of the separator. Figures 7 and 8 show the experiment results.

Figure 7a–c shows the ash ratio (%) (percentage of ash to raw coal), coal ratio (%) (percentage of coal to raw coal), and sulfur ratio (%) (percentage of sulfur to each tray) of the collected particles from each tray at conveyor speeds ( $V_1$ ) of 23, 48, and 73 g/min. The ash removal ratio, combustible matter recovery ratio, and separation efficiency at a conveyor speed of 23 g/min were slightly higher than those of conveyor speed of 48 g/min (Figure 8a,b), and the ash removal ratio, the combustible matter recovery ratio, and the separation efficiency at a conveyor speed of 73 g/min were markedly lower than those of conveyor speeds of 23 and 48 g/min.

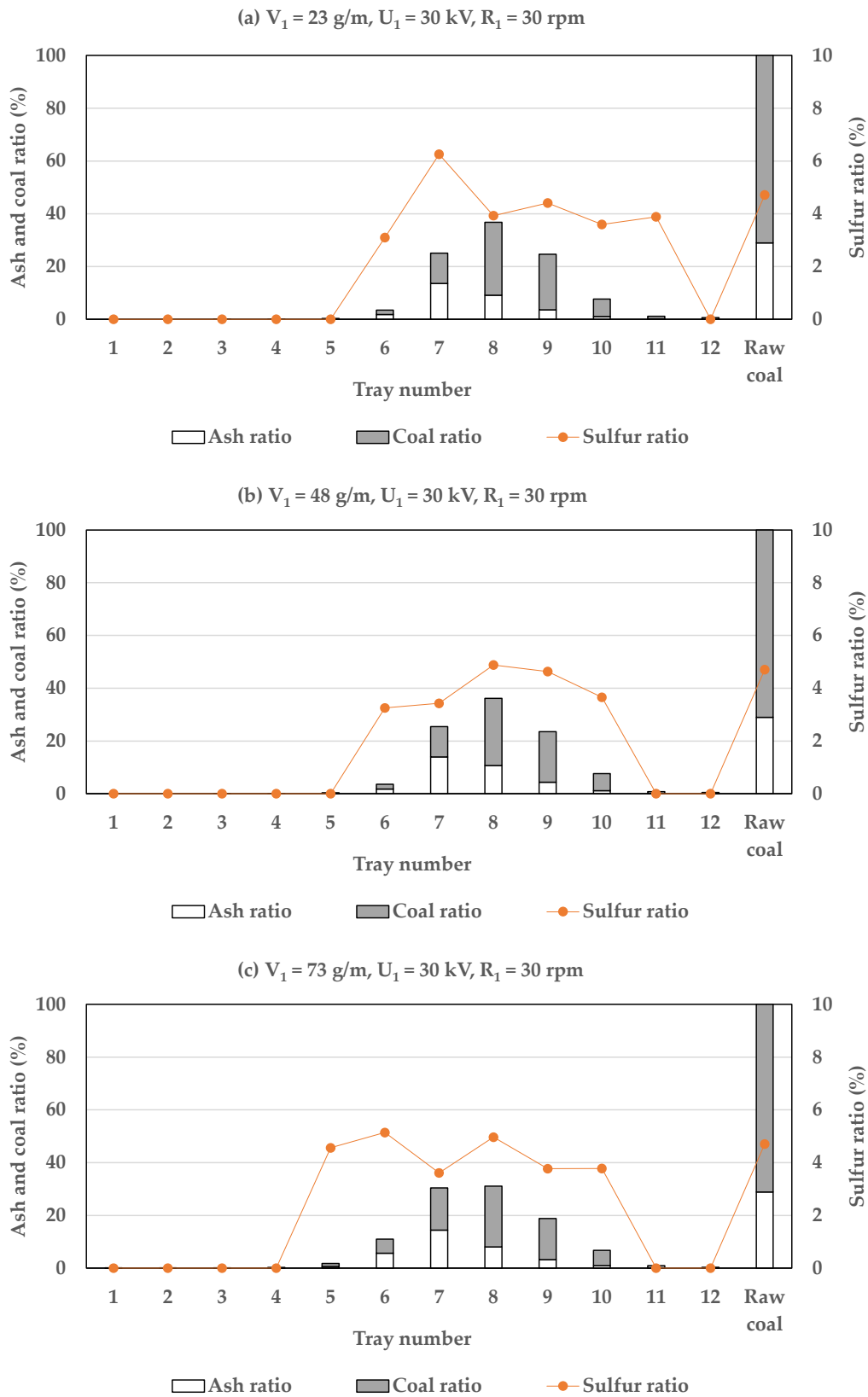


**Figure 7.** Ash ratio (%), coal ratio (%), and sulfur ratio (%) of the particles collected from the 12 trays at different conveyor speeds: (a) 23 g/min; (b) 48 g/min; (c) 73 g/min using a dry coal cleaning system with two-stage corona electrostatic processes.

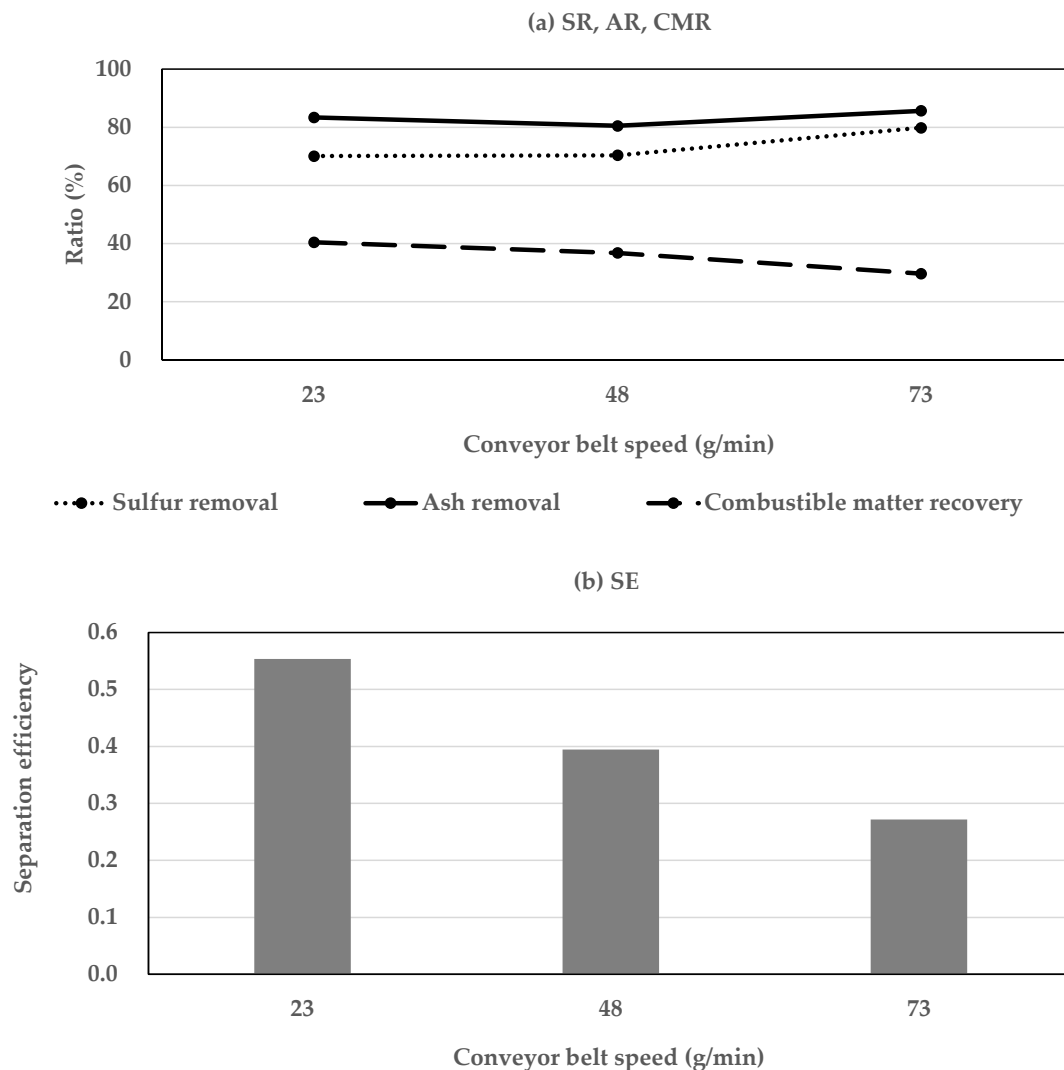


**Figure 8.** Performance of the separator at different conveyor speeds: (a) ash removal ratios (%), sulfur removal ratios (%), and combustible matter recovery ratios (%); (b) efficiencies of coal separation using a dry coal cleaning system with two-stage corona electrostatic processes.

It is reasonable to conclude that a larger feeding speed leads to poorer performance such as a lower clean coal recovery ratio and a higher ash content of the clean coal from Figures 7 and 8. An excessively high conveyor speed results in some feedstock particles not being fully electrically charged in the electrical field because of the thick layer and some particles not coming into full contact with the drum surface, as a result, these particles are subjected a small electric force compared to a large centrifugal force and gravity force and then fall into the left trays, resulting in a lower clean coal recovery ratio.

### 3.2. Efficiency of Two-Stage Coal Separation

In order to improve the separation efficiency, we conducted a two-stage separation process experiment based on the experimental results described above. In the process, the middling particles of the first stage were given to the second stage to separate, the second stage experiment conditions are as follows: drum rotational speed ( $R_2$ ) of 30 rpm, distance ( $S_2$ ) of 7 cm, electrode angle ( $\theta_2$ ) of  $75^\circ$ , temperature of  $25^\circ\text{C}$ , relative humidity of 60%, and feedstock size range of 0.5–1 mm. The total yield of clean coal of the two stages was considered as the final efficiency of the two-stage process. Figures 9 and 10 show the results. Figure 9a,b shows the results of the first and second stages of separation, respectively.

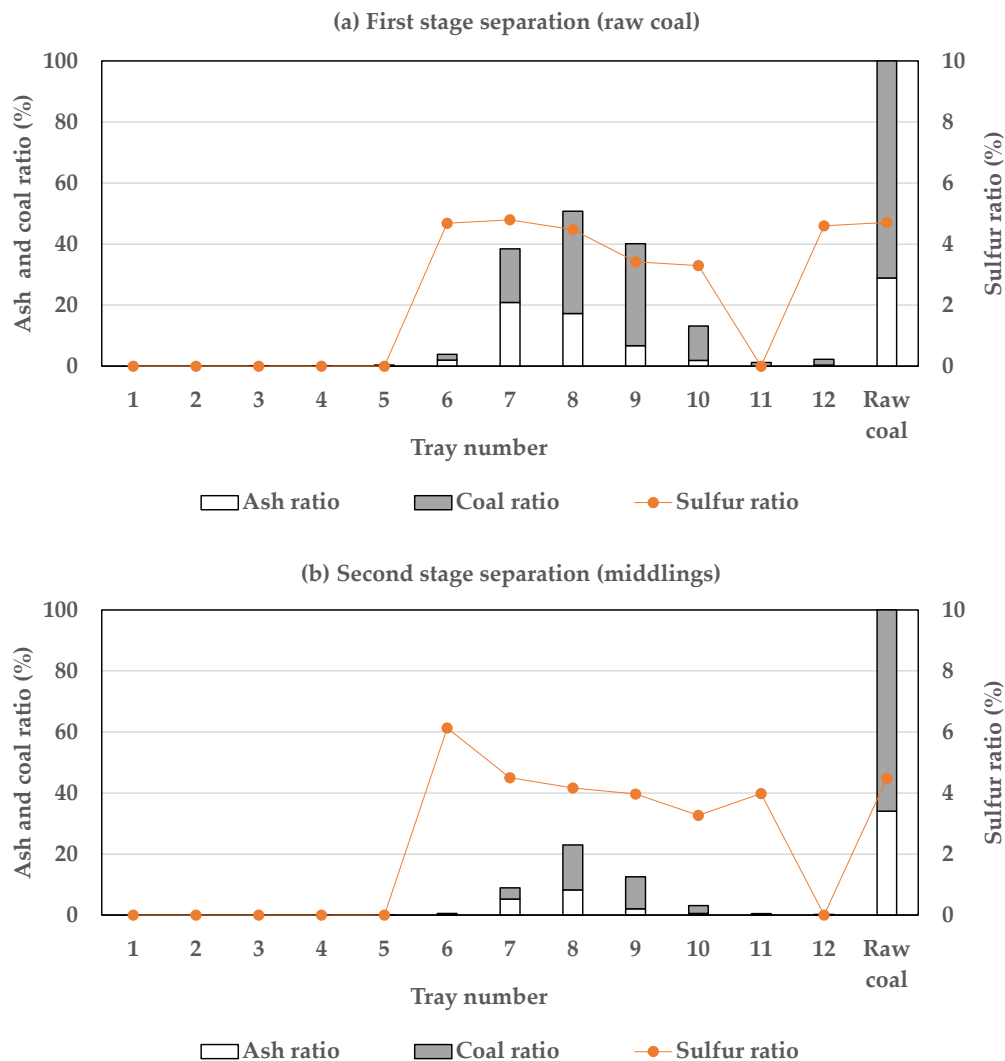


**Figure 9.** The results of a dry coal cleaning system with two-stage corona electrostatic processes: (a) the first stage of cleaning; (b) the second stage of cleaning.

The clean coal recovery ratio (particles collected from tray numbers 9–12) of the first stage was 37.80% (Figure 9a). The middlings (particles collected from tray number 8) accounted for 33.78% by weight of the feedstock and had an ash content of 34.04%. The middlings were fed to the second separator for the second stage of cleaning. The results are shown in Figure 9b. The second stage process will produce 46.84% middlings, higher than that of the first stage, but will produce a higher clean coal recovery ratio of 33.00% (Figure 9b).

The first-stage separation of dry coal cleaning system achieved a lower ash removal ratio but a higher combustible matter recovery ratio than that of the second-stage separation (Figure 10a). The separation efficiencies of the first and second stages were 0.69 and 0.61, respectively (Figure 10b), therefore, the second stage separation was also very effective. The overall performance of two stage separation process was calculated by combining the data in Figure 10a,b. The combustible matter recovery ratio and overall separation efficiency of two stage process were markedly improved compared with that of the single-stage process.

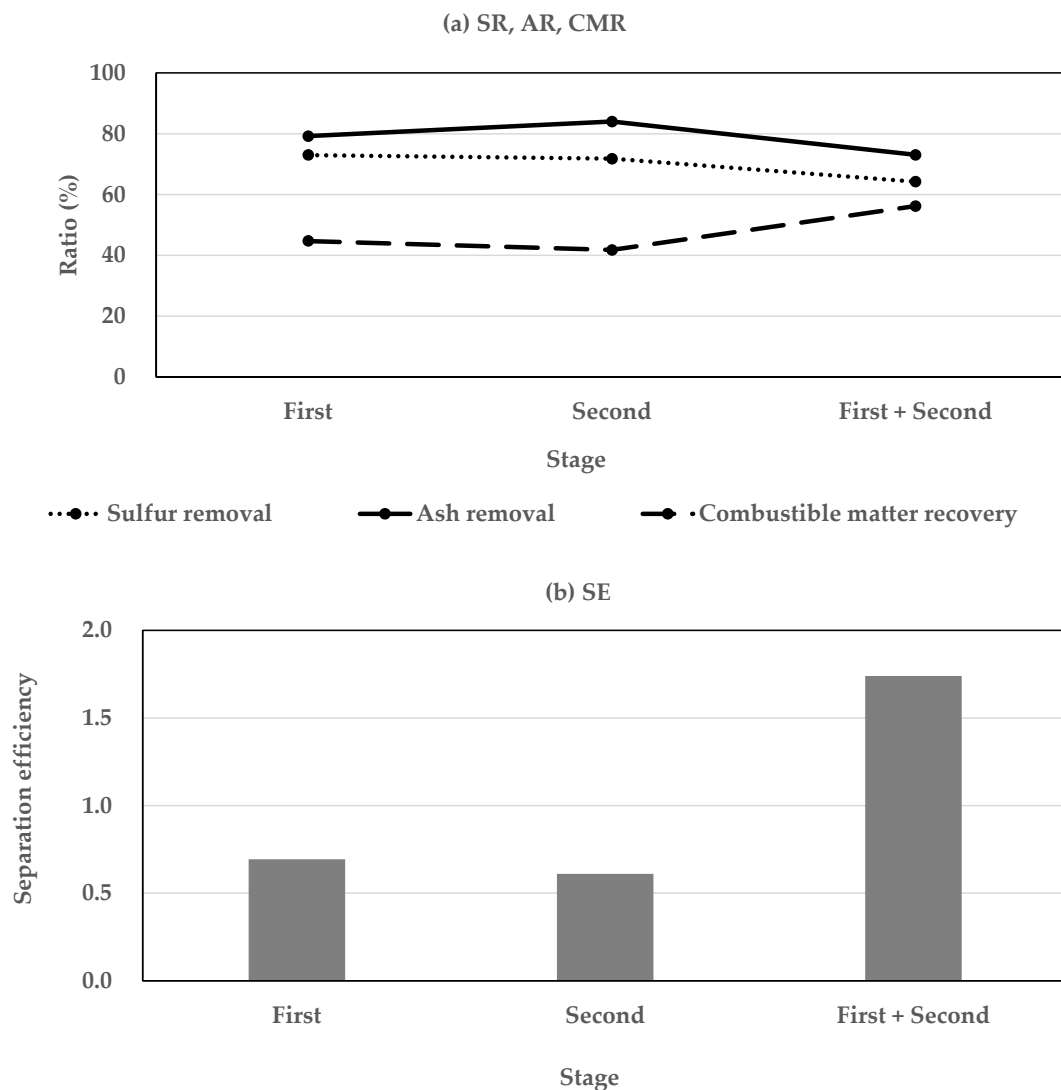


**Figure 10.** Performance of two-stage coal cleaning: (a) ash removal ratio (%), sulfur removal ratio (%), and combustible matter recovery ratio (%); (b) efficiency of coal separation using a dry coal cleaning system with two-stage corona electrostatic processes.

### 3.3. Comparative Analysis of the Composition and Properties of the High-Sulfur Raw Coal and Clean Coal

#### 3.3.1. Combustion Behavior

The optimum conditions for voltage ( $U_1$ ), distance ( $S_1$ ), and angle ( $\theta_1$ ) were discussed above (Section 3.1); these are 30 kV, 7 cm, and  $75^\circ$ , respectively. After separation, the quality of clean coal accounted for 48.41% of the raw coal mass, the proximate analysis results of clean coal show that the ash content decreases from 38.60 to 18.71%, the volatile matter content increases from 33.20% to 44.60%, and the water content increases from 2.90 to 10.11%. It is seen that the ash content in clean coal decreases significantly, which indicates that the raw coal is converted from high-ash coal to low-ash coal.

Figure 11a,b shows the mass loss rates at different temperatures. At temperatures in the range of 25–200 °C, the mass losses involved only moisture evaporation. The clean coal had a larger maximum mass loss rate and a higher burn-out temperature, which indicates that the clean coal was more combustible than raw coal and has a great calorific value. The mass loss–temperature curve exhibits a small peak at 450 °C and it is reasonable to conclude that this small peak is due to the rapid combustion of the sulfur from the data shown in Figure 12a.

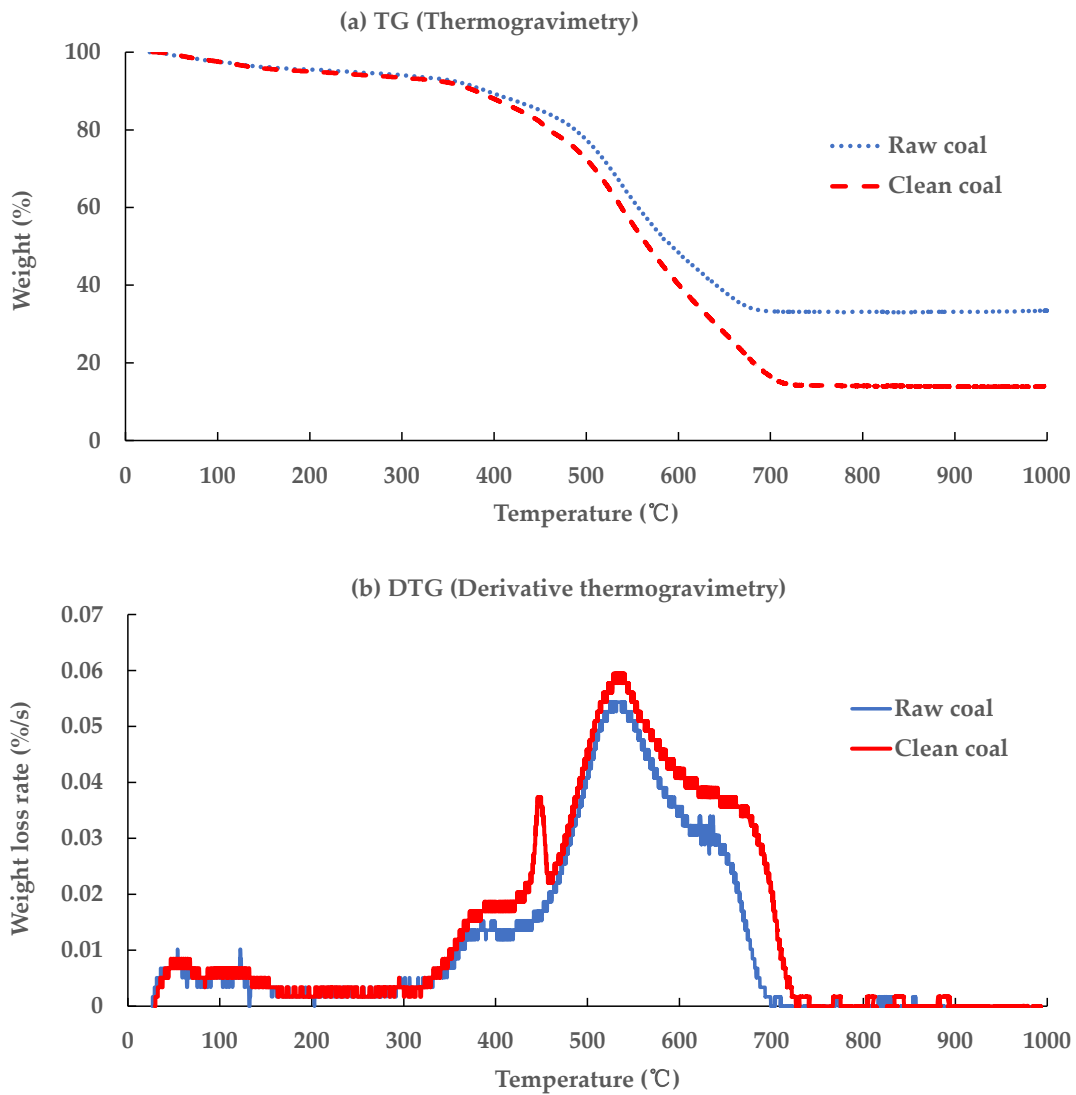


**Figure 11.** Combustion behavior of the raw coal and its clean coal using a dry coal cleaning system with two-stage corona electrostatic processes. (a) TG (thermogravimetry); (b) DTG (derivative thermogravimetry).

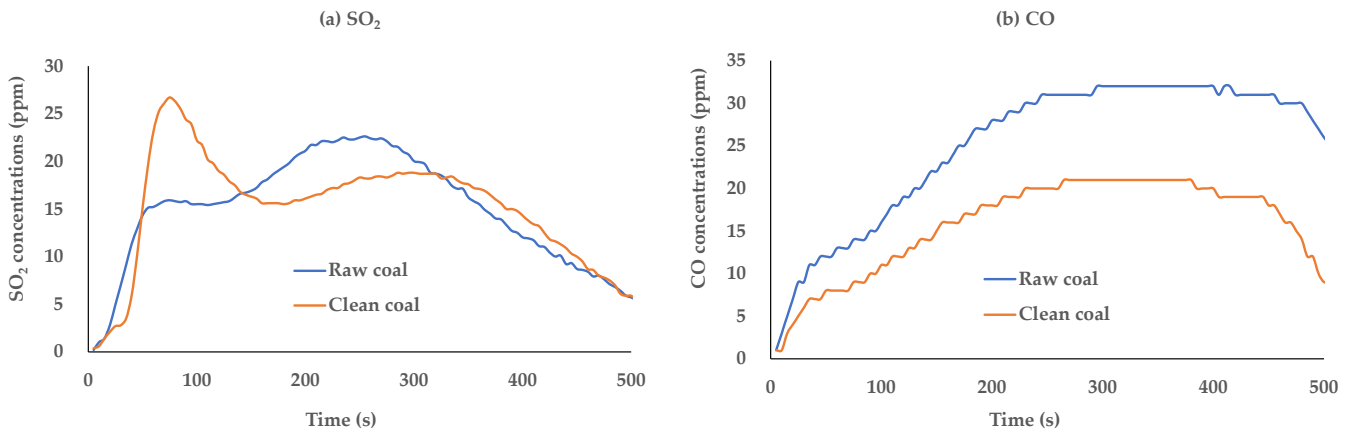


**Figure 12.** Cont.

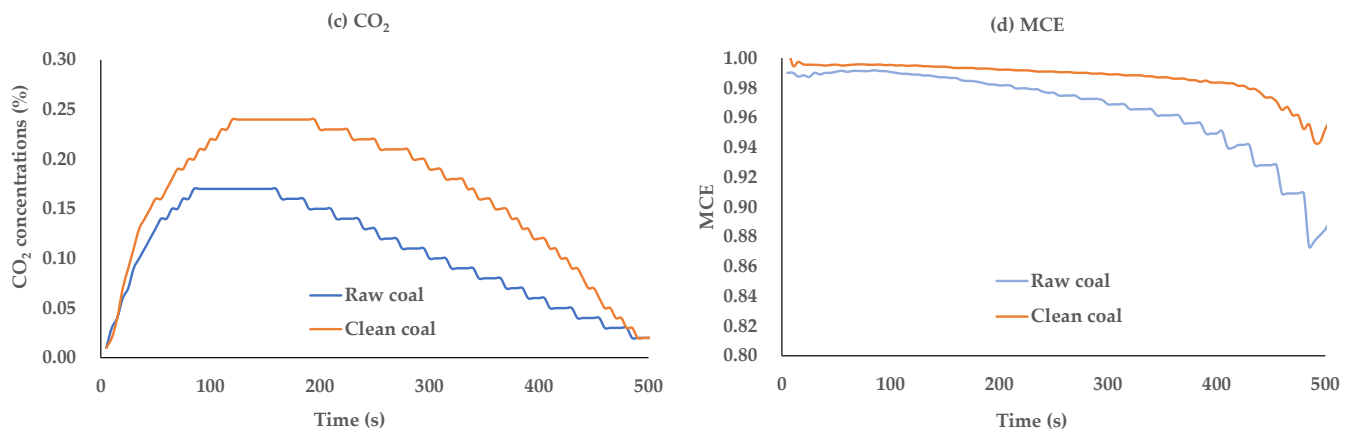


**Figure 12.** Air pollutant emissions of (a) the concentration of SO<sub>2</sub>; (b) the concentration of CO; (c) the concentration of CO<sub>2</sub>; (d) the modified combustion efficiency from the combustion of the raw coal and its clean coal using a dry coal cleaning system with two-stage corona electrostatic processes.

### 3.3.2. Experimental Investigation of Air Pollutant Emissions

The air pollutant emissions from the combustion of the raw coal and clean coal were experimentally investigated by burning 200 mg samples of raw coal and clean coal at the temperature of 850 °C and airflow rate of 5 L/min. Figure 12 shows the amounts of air pollutant emissions. Figure 12a shows the variation of SO<sub>2</sub> concentration with time during the process of combustion. It can be seen that the clean coal released more sulfur from the 50th to 150th second than the raw coal based on surveying data using TG-DTA analyzer, it is because the organic sulfur in clean coal is higher than that in raw coal, and the organic sulfur will easily burn at a lower temperature, and clean coal will release less CO in the combustion process because of complete combustion, and clean coal released more CO<sub>2</sub> in the combustion process (Figure 12c) because clean coal had a larger combustible ratio than that of raw coal, which is consistent with the results presented in Figure 12b. Clean coal had a higher modified combustion efficiency (MCE: CO<sub>2</sub>/CO<sub>x</sub>) (Figure 12d) because of more complete combustion.

## 4. Conclusions

The experimental results show that the factors of electrode voltage, drum rotational speed, and feedstock feeding speed of the corona separator had marked influences on the performance of the separation process, and this dry coal cleaning system with two-stage corona electrostatic processes can effectively reduce the ash content of the coal and performs much better than single-stage separation processes. Under the experimentally determined optimal parametric settings, the process can reduce ash content from 28.92% (raw coal) to 16.32% (clean coal) and sulfur content reduced from 4.71% to 3.53%. The sulfur content of the raw coal could not be further reduced because of organic sulfur associated with clean coal and concentrated in clean coal, and no physical methods can effectively remove this proportion of the organic sulfur.

The combustion behavior of raw coal and the clean coal and the air pollutant emissions released from the combustion of the raw and clean coals were comparatively analyzed. The results show that clean coal was a better fuel for combustion, the clean coal burned more completely and resulted in fewer CO emissions. This experimental study provides a simple and feasible approach to dry coal cleaning that is particularly well suited to preliminary coal cleaning in the power stations.

Finally, this study has its limitations. Firstly, corona electrostatic separation is a physical separate method, and the sub-method can only reject inorganic sulfur in raw coal, but not organic sulfur effectively, therefore, it is not effective for raw coals with high organic sulfur content. Secondly, because the charged properties of coal and ash vary

significantly for different raw coals, the optimal separate conditions of each raw coal need to be confirmed, so it is not possible to screen multiple raw coals simultaneously. In the future, it will be a very interesting topic to confirm the electrical properties and density of different substances in the raw coal, and hopefully find the better method of electric coal cleaning system.

**Author Contributions:** The manuscript was written through contributions of all authors. All authors have given approval to the final version of the manuscript. Conceptualization: C.L. and Q.W.; methodology: Q.W. and C.L.; software: C.L.; validation: Q.W.; formal analysis: C.L.; investigation, C.L. and Q.W.; resources: Q.W.; data curation: C.L.; writing—original draft preparation: C.L.; writing—review and editing, Q.W.; visualization: C.L.; supervision, Q.W.; project administration, Q.W. All authors have read and agreed to the published version of the manuscript.

**Funding:** This study was partially supported by the special funds for Basic Research (B) (No. 15H05119, 376 FY2015~FY2017) of Grant-in-Aid Scientific Research of the Japanese Ministry of Education, Culture, Sports, 377 Science and Technology (MEXT), Japan.

**Acknowledgments:** We would like to thank Xinxi Zhang of China University of Mining & Technology for his kind indication and help during reviewing and editing this article.

**Conflicts of Interest:** The authors declare no conflict of interest. The funder had no role in the design of the study; in the collection, analyses, or interpretation of data; in the writing of the manuscript, or in the decision to publish the results.

## Abbreviations

SR	Sulfur removal
AR	Ash removal
CMR	Combustible matter recover
SE	Separation efficiency
$Wt_{feed}$	Mass of raw coal supply
$Wt_{clean}$	Mass of recovery of clean coal
$Sulfur_{feed\ ratio}$	Mass of sulfur rate of raw coal
$Sulfur_{clean\ ratio}$	Mass of sulfur rate of clean coal
U	Electrode voltages
S	Distance between the electrode and the drum
$\theta$	Angle between the line from the electrode to the center of the drum circle and the vertical line of the drum
T	Room temperature
RH	Relative humidity
R	Drum rotational speed
V	Conveyor speed
rpm	Revolution(s) Per Minute
g/m	Grams Per Minute
M	Moisture
V.M	Volatile matter
F.C	Fixed carbon
$A_d$	Ash content
Sd	Sulfur content
COx	Oxocarbon
SOx	Sulfur oxides
TG	Thermogravimetry
DTG	Derivative thermogravimetry
L/min	Liters Per Minute

## References

1. Petroleum, B. *BP Statistical Review of World Energy Report*; BP: London, UK, 2019.
2. Wang, D.; Ding, R.; Gong, Y.; Wang, R.; Wang, J.; Huang, X. Feasibility of the Northern Sea Route for oil shipping from the economic and environmental perspective and its influence on China's oil imports. *Mar. Policy* **2020**, *118*, 104006. [[CrossRef](#)]
3. Zeng, S.; Gu, J.; Yang, S.; Zhou, H.; Qian, Y. Comparison of techno-economic performance and environmental impacts between shale gas and coal-based synthetic natural gas (SNG) in China. *J. Clean. Prod.* **2019**, *215*, 544–556. [[CrossRef](#)]
4. Hache, E. Do renewable energies improve energy security in the long run? *Int. Econ.* **2018**, *156*, 127–135. [[CrossRef](#)]
5. Li, J.; Hu, S. History and future of the coal and coal chemical industry in China. *Resour. Conserv. Recycl.* **2017**, *124*, 13–24. [[CrossRef](#)]
6. Meshram, P.; Purohit, B.K.; Sinha, M.K.; Sahu, S.K.; Pandey, B.D. Demineralization of low grade coal—A review. *Renew. Sustain. Energy Rev.* **2015**, *41*, 745–761. [[CrossRef](#)]
7. Xie, X.; Liu, X.; Wang, H.; Wang, Z. Effects of aerosols on radiative forcing and climate over East Asia with different SO<sub>2</sub> emissions. *Atmosphere* **2016**, *7*, 99. [[CrossRef](#)]
8. Kaufmann, R.K.; Kauppi, H.; Mann, M.L.; Stock, J.H. Reconciling anthropogenic climate change with observed temperature 1998–2008. *Proc. Natl. Acad. Sci. USA* **2011**, *108*, 11790–11793. [[CrossRef](#)] [[PubMed](#)]
9. Qiao, H.; Chen, S.; Dong, X.; Dong, K. Has China's coal consumption actually reached its peak? National and regional analysis considering cross-sectional dependence and heterogeneity. *Energy Econ.* **2019**, *84*, 104509. [[CrossRef](#)]
10. Qian, Y.; Scherer, L.; Tukker, A.; Behrens, P. China's potential SO<sub>2</sub> emissions from coal by 2050. *Energy Policy* **2020**, *147*, 111856. [[CrossRef](#)]
11. Su, S.; Li, B.; Cui, S.; Tao, S. Sulfur dioxide emissions from combustion in China: From 1990 to 2007. *Environ. Sci. Technol.* **2011**, *45*, 8403–8410. [[CrossRef](#)] [[PubMed](#)]
12. Shammas, N.K.; Wang, L.K.; Wang, M.H.S. Sources, chemistry and control of acid rain in the environment. In *Handbook of Environment and Waste Management: Acid Rain and Greenhouse Gas Pollution Control*; World Scientific Publishing Co.: Singapore, 2020; pp. 1–26. [[CrossRef](#)]
13. Yu, S.; Zhang, C.; Yuan, C.; Xu, H.; Ma, L.; Fang, Q.; Chen, G. Investigation on the influence of sulfur and chlorine on the initial deposition/fouling characteristics of a high-alkali coal. *Fuel Process. Technol.* **2020**, *198*, 106234. [[CrossRef](#)]
14. Breeze, P. Combustion plant emissions: Sulfur dioxide, nitrogen oxides, and acid rain. In *Electricity Generation and the Environment*; Elsevier: Amsterdam, The Netherlands, 2017. [[CrossRef](#)]
15. Chen, Q.; Sun, H.; Wang, J.; Shan, M.; Yang, X.; Deng, M.; Zhang, L. Long-life type—The dominant fraction of EPFRs in combustion sources and ambient fine particles in Xi'an. *Atmos. Environ.* **2019**, *219*, 117059. [[CrossRef](#)]
16. Yuegang, T.; Xin, H.; Aiguo, C.; Wei-wei, L.; Xiu-jie, D.; Qiang, W.; Long, L. Occurrence and sedimentary control of sulfur in coals of China. *J. China Coal Soc.* **2015**, *40*, 1976–1987. [[CrossRef](#)]
17. Cai, S.; Zhang, S.; Wei, Y.; Sher, F.; Wen, L.; Xu, J.; Dang, J.; Hu, L. A novel method for removing organic sulfur from high-sulfur coal: Migration of organic sulfur during microwave treatment with NaOH-H<sub>2</sub>O<sub>2</sub>. *Fuel* **2021**, *289*, 119800. [[CrossRef](#)]
18. Wang, F.; Liu, B.; Zhang, B. Embodied environmental damage in interregional trade: A MRIO-based assessment within China. *J. Clean. Prod.* **2017**, *140*, 1236–1246. [[CrossRef](#)]
19. Cheng, G.; Zhang, C. Desulfurization and Denitrification Technologies of Coal-fired Flue Gas. *Pol. J. Environ. Stud.* **2018**, *27*, 481–489. [[CrossRef](#)]
20. Tripathy, S.K.; Ramamurthy, Y.; Kumar, C.R. Modeling of high-tension roll separator for separation of titanium bearing minerals. *Powder Technol.* **2010**, *201*, 181–186. [[CrossRef](#)]
21. Higashiyama, Y.; Asano, K. Recent progress in electrostatic separation technology. *Part. Sci. Technol.* **1998**, *16*, 77–90. [[CrossRef](#)]
22. Iuga, A.; Dăscălescu, L.; Morar, R.; Csorvassy, I.; Neamiu, V. Corona-electrostatic separators for recovery of waste non-ferrous metals. *J. Electrostat.* **1989**, *23*, 235–243. [[CrossRef](#)]
23. Venter, J.A.; Vermaak, M.K.G.; Bruwer, J.G. Influence of surface effects on the electrostatic separation of zircon and rutile. *J. S. Afr. Inst. Min. Metall.* **2008**, *108*, 55–60.
24. Veit, H.M.; Diehl, T.R.; Salami, A.P.; Rodrigues, J.D.S.; Bernardes, A.M.; Tenório, J.A.S. Utilization of magnetic and electrostatic separation in the recycling of printed circuit boards scrap. *Waste Manag.* **2005**, *25*, 67–74. [[CrossRef](#)] [[PubMed](#)]
25. Tilmatine, A.; Medles, K.; Younes, M.; Bendaoud, A.; Dascalescu, L. Roll-type versus free-fall electrostatic separation of tribocharged plastic particles. *IEEE Trans. Ind. Appl.* **2010**, *46*, 1564–1569. [[CrossRef](#)]
26. Zhang, X. Study on Desulfurization and Ash Reduction of fine Coal. *D. Xuzhou China Univ. Min. Technol.* **1994**.
27. Liu, C.; Wang, Q. Study on Electrostatic Preparation High-Ash Coal from China Using Roll-Type Electrostatic Separator and the Combustion Characteristics of the Cleaned Coal. *Processes* **2021**, *9*, 1139. [[CrossRef](#)]
28. Wang, Q.; Sarkar, J.k. Investigations of the pyrolysis behaviors of coconut shell and husk waste biomasses. *Int. J. Energy Prod. Manag.* **2018**, *3*, 34–43. [[CrossRef](#)]
29. Lazaroiu, G.; Pop, E.; Negreanu, G.; Pisa, I.; Mihaescu, L.; Bondrea, A.; Berbece, V. Biomass combustion with hydrogen injection for energy applications. *Energy* **2017**, *127*, 351–357. [[CrossRef](#)]